

# UC Berkeley

## UC Berkeley Previously Published Works

### Title

Fallout melt debris and aerodynamically-shaped glasses in beach sands of Hiroshima Bay, Japan

### Permalink

<https://escholarship.org/uc/item/6tk816t9>

### Authors

Wannier, Mario MA  
de Urreiztieta, Marc  
Wenk, Hans-Rudolf  
[et al.](#)

### Publication Date

2019-03-01

### DOI

10.1016/j.ancene.2019.100196

Peer reviewed

# Fallout melt debris and aerodynamically-shaped glasses in beach sands of Hiroshima Bay, Japan

Mario M.A. Wannier<sup>a,\*</sup>, Marc de Urreiztieta<sup>b</sup>, Hans-Rudolf Wenk<sup>c</sup>, Camelia V. Stan<sup>d</sup>, Nobumichi Tamura<sup>d</sup>, Binbin Yue<sup>c,d</sup>

<sup>a</sup> F2 Park Seven Condominium, 50450 Kuala Lumpur, Malaysia

<sup>b</sup> Rue J.G de Mauduit 5, 29300 Quimperlé, France

<sup>c</sup> Dept. Earth and Planetary Science, University of California, Berkeley CA 94720, USA

<sup>d</sup> Advanced Light Source, Lawrence Berkeley National Laboratory, Berkeley CA 94720, USA

## ABSTRACT

A complex association of millimeter-sized, aerodynamically-shaped debris, including glass spherules, glass filaments, and composite-fused melt particles was recovered from beach sands on the shores of the Motoujina Peninsula in Hiroshima Bay, Japan. Based on optical microscopy, this debris comprises six morphological groups ranging from clear glasses to rubber-like constituents. Scanning electron microscopy and synchrotron X-ray microdiffraction revealed dominant aluminum, silicon and calcium (Al-Si-Ca) elemental composition with some iron, mainly in glass, associated with precipitates of mullite and anorthite microcrystals, hematite dendrites and iron-chromium globules, indicative of original temperature conditions >1800 °C. Aerodynamically-shaped fallout debris, including glass spherules described in this study, are generally produced by single high-energy catastrophic events, such as an extraterrestrial body impacting Earth or a nuclear explosion. This study interprets the large volumes of fallout debris generated under extreme temperature conditions as products of the Hiroshima August 6th, 1945 atomic bomb aerial detonation. The chemical composition of the melt debris provides clues to their origin, particularly with regard to city building materials. This study is the first published record and description of fallout resulting from the destruction of an urban environment by atomic bombing.

## 1. Introduction

Geological and anthropogenic processes can produce "fallout" deposited at a distance from its source. Meteorite impacts can lead to ejection of melted (and/or shocked) rocks, for example, deposited at great distances from the impact site. Most such ejecta are crystalline, but some are glassy (representing rock melt from the upper continental crust), such as impact glasses and tektites that occur as mostly macroscopic (centimeter-sized) objects, as well as, for three of the four known strewn fields, submillimeter-sized microtektites (e.g., [Stöffler and Grieve, 2007](#); [French and Koeberl, 2010](#), and [Koeberl, 2014](#), and references therein). Volcanic eruptions generating suspension pyroclastic fall deposits can also produce distal fallout (e.g. [Morgan and Schulz,](#)

[2012](#)). Anthropogenic actions such as fireworks (e.g., [Grima et al., 2011](#)), industrial contaminants, and nuclear explosions (e.g., [Miller, 1964](#); [Weisz et al., 2017](#)) can also produce similar debris. Fallout debris from nuclear explosions consist of spherules and aerodynamically-shaped glasses, created aerially by high-velocity quenching processes involving materials melted and vaporized at temperatures in the order of 2000 °C.

During a sedimentological and microfaunal pilot study of the Hiroshima Bay, Japan, we collected 13 intertidal modern sand samples from six beaches to the East, South and West of Motoujina Peninsula ([Figs. 1 & S1a](#); [Table S1](#)). We took samples from the surface to a depth of about 10 cm on the exposed beaches, where the recent faunal components accumulate. While analyzing the sands, we detected a rich and diverse association of spherules, other aerodynamically-shaped glasses and a variety of melt debris ([Figs. 2 & S1b](#)). These "Motoujina Fallout Debris" (MFD) stand out as smooth, rounded and often fragile particles among the coarse quartzitic and feldspathic sedimentary particles that form the natural beach sands. Four other beach sand samples from the nearby island of Miyajima ([Fig. 1](#); [Table S2](#)) also revealed the

Abbreviation: MFD, Motoujina Fallout Debris.

\* Corresponding author. Present address: Chemin des Vignes 5, 1806 Saint L gier-La Chi saz, Switzerland.

E-mail address: [mwannier@yahoo.com](mailto:mwannier@yahoo.com) (M.M.A. Wannier).

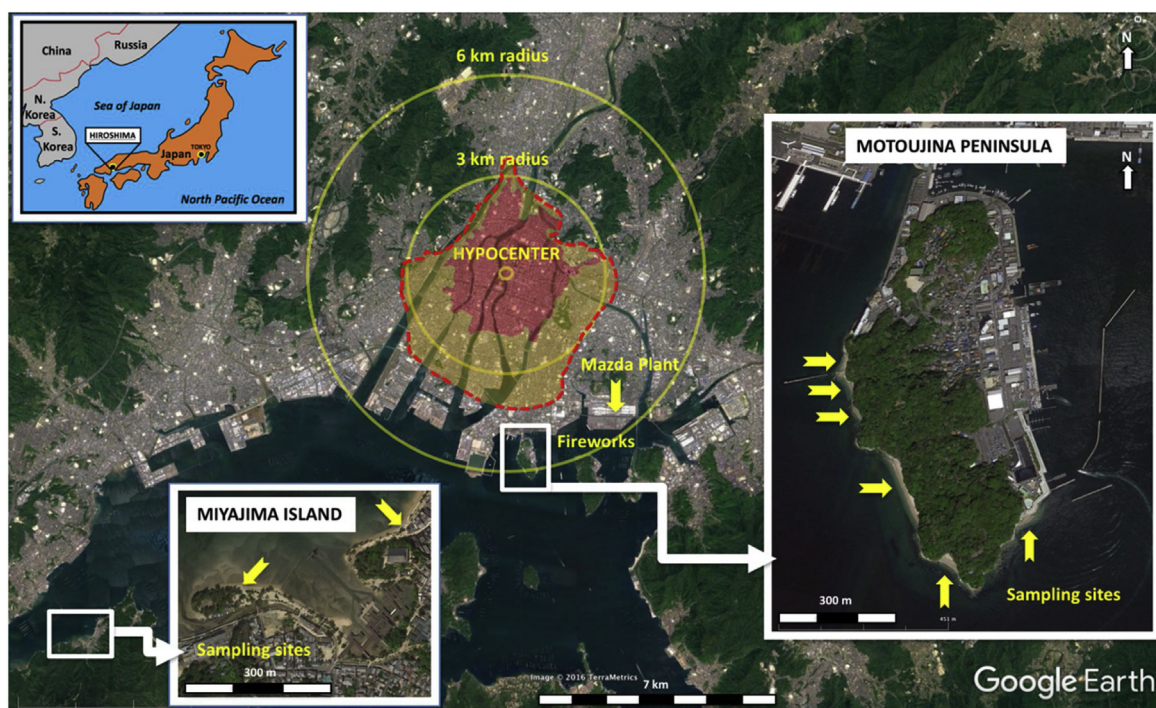


**Fig. 1.** Hiroshima city and bay area with location of the A-bomb hypocenter. The red polygon shows the extent of the fire; the yellow polygon and red dashed line indicate the extent of structural damage. The figure also indicates the locations where the Mazda plant fire occurred, and the yearly firework festival takes place. Inset maps: sampling sites at Motoujina Peninsula and Miyajima Island (Refer to Supplementary Tables S1, S2 & S6 for geographical coordinates).

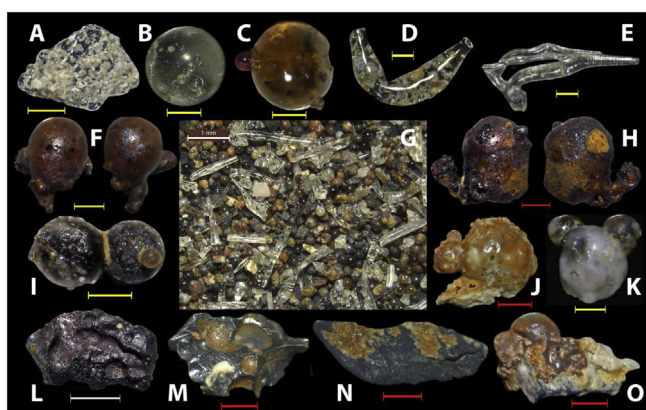


**Fig. 2.** Optical microscopy images of selected Motoujina fallout debris. (A) Vesicular glass shard, (B) clear, vesicular glass spherule, (C) large glassy spherule with fused smaller spherules, (D) bent vesicular glass filament, (E) glass filaments complex, (F) amalgamated opaque spheroids (opposite views of the same specimen), (G) tray content, fine sand fraction of one rich sample, (H) complex, amalgamated opaque particle (opposite views of the same specimen), (I) fused and cemented opaque spherules covered with a thin glass layer, (J) agglomerated, melt-covered debris, (K) larger spherule with fused smaller spherules, all covered by an opaque surface melt, (L) rubber-like debris, (M) ferro-magnetic debris with a cratered surface, (N) meta-sediment debris with patches of glass melt, (O) melt-covered meta-sediment debris with magnetic, half spherical body. White scale bar: 1 mm; red scale bar: 500  $\mu\text{m}$ ; yellow scale bar: 200  $\mu\text{m}$ .

presence of similar particles, though in significantly lower abundance and diversity, and mostly restricted to the very fine sand and silt fractions.

The yet unreported presence of fallout debris at Hiroshima Bay, respectively six and twelve km away from the Hiroshima A-bomb hypocenter (Fig. 1) prompted this study. Are these debris related to the Hiroshima August 6th, 1945 atomic bomb aerial detonation? To

what extent can other natural or human phenomenon explain the occurrence of melt debris and aerodynamically-shaped particles in the Hiroshima Bay? In this study we investigate the petrography of the samples and use optical microscopy, scanning electron microscopy (SEM) and synchrotron X-ray microdiffraction. We compare MFD with micrometeorites, cosmic spherules, cosmic airbursts, microtektites, volcanic glasses, firework and industrial melt debris and debris particles from nuclear explosion. The results strongly support the hypothesis that the Motoujina fallout debris were formed during the atomic bomb explosion.

## 2. Methods

Dried samples of beach sand from Hiroshima Bay ranging from 60 and 130 g in weight, are sieved in seven fractions representing Wentworth grain-size classes, including granules, very coarse sand, coarse sand, medium sand, fine sand, very fine sand and silt and clay (see Supplementary Text (a)). Sample material from each fraction is then spread on a gridded picking tray and examined under reflected light at magnifications of 25x to 80x with a Greenough stereo microscope, Leica S9 APO with apochromatic 8:1 zoom and 75 mm working distance. All melt debris are systematically separated, counted, photographed and the examined material weighed (Table S3). In this process, the total number of sediment grains examined on the tray is counted where practical, or estimated in upscaling grain counts for a few grid cells (Table S4). Our dataset comprises over 10,000 MFD, out of which some 9595 particles were systematically counted and separated into morphological groups, providing the foundation for a semi-quantitative abundance analyses based on granulometric classes (Table S5). With a magnet reacting particles are identified.

Microstructures of fifteen samples representing the various groups are analyzed with a Zeiss-EVO MA10 Scanning Electron Microscope (SEM) at EPS UC Berkeley to characterize microstructures. The SEM was operating at low vacuum conditions at

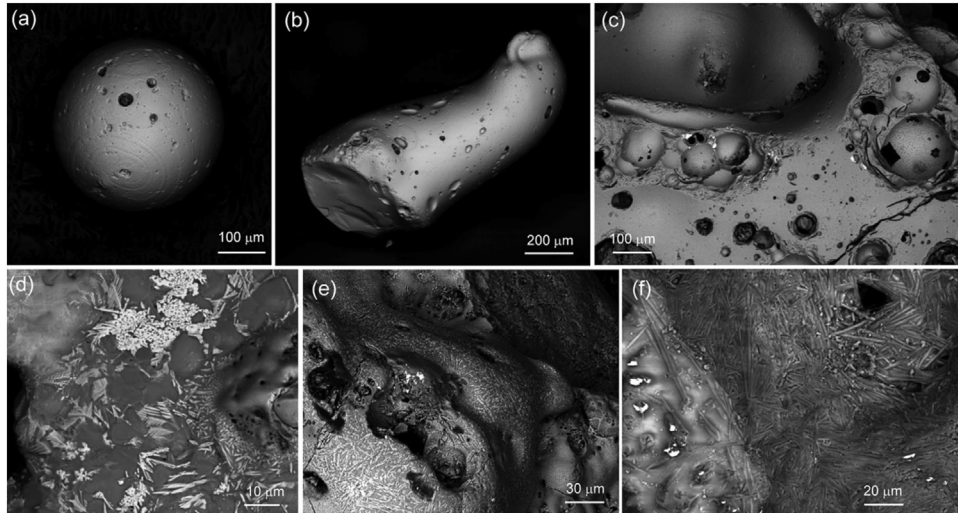


**Fig. 3.** Scanning Electron Microscopy (SEM) backscatter images of selected Motoujina fallout debris. (a) Clear sphere, (b) clear filament, (c) flow structures with bubbles, bright spots are iron (Fe)-chromium (Cr) alloy, (d) dendritic structures of iron-oxide, (e) flow structures with white iron-oxide crystals, (f) Needle-like crystals of aluminum (Al)-iron (Fe)-silicon (Si) oxide composition in a silicon-aluminum-calcium oxide matrix; bright spots are Fe-Cr.

20kV, in order to avoid carbon coating and being able to analyze samples for carbon and oxygen. SEM-Backscatter electron (BE) images of six samples are displayed in Fig. 3. The brightness contrast is indicative of compositional differences. Chemical analyses with an EDAX energy dispersive spectroscopy system (EDS) provide estimates about chemical composition. Fig. 4 shows some SEM-EDS spectra.

Because of the small sample size and the high heterogeneity at the micron-scale (Fig. 3), conventional X-ray powder diffraction is not useful to identify individual phases. Therefore, we applied synchrotron X-ray micro-diffraction to identify phases based on

their diffraction patterns (Fig. 5). We performed the synchrotron experiments on four samples out of the 15 samples studied by SEM at the Advanced Light Source, Lawrence Berkeley National Laboratory, with a  $5 \times 2 \mu\text{m}^2$  monochromatic beam (1.23986 Å wavelength). The X-ray diffraction patterns are collected in transmission geometry on particles mounted on glass rods, using an area detector (DECTRIS Pilatus 1 M) positioned at a  $40^\circ$  angle with respect to the incident X-ray direction and at a distance of approximately 185 mm from the sample. The XMAS software (Tamura, 2014) is used to integrate the diffraction images along the azimuthal direction into 1D diffractograms.

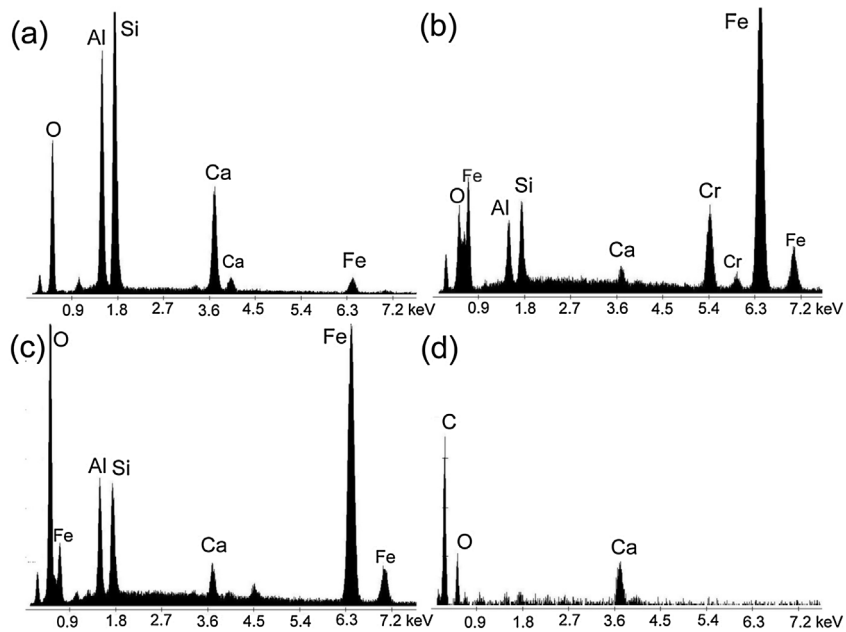


**Fig. 4.** Scanning Electron Microscopy / Energy Dispersive X-Ray Spectroscopy (SEM-EDS) spectra of Motoujina fallout debris fragments. (a) Composition of clear glass spherules (Fig. 3a, b); (b) droplets of metallic Fe-Cr, probably representative of stainless steel (Fig. 3c); (c) dendritic Fe-oxide of hematite structure in Al-Si-Ca matrix (Fig. 3d); (d) carbon (C)-oxygen (O) rich composition of rubber-like particles (Fig. 3d). Note that dendritic crystallites are very small and signals from the surrounding matrix cannot be excluded.

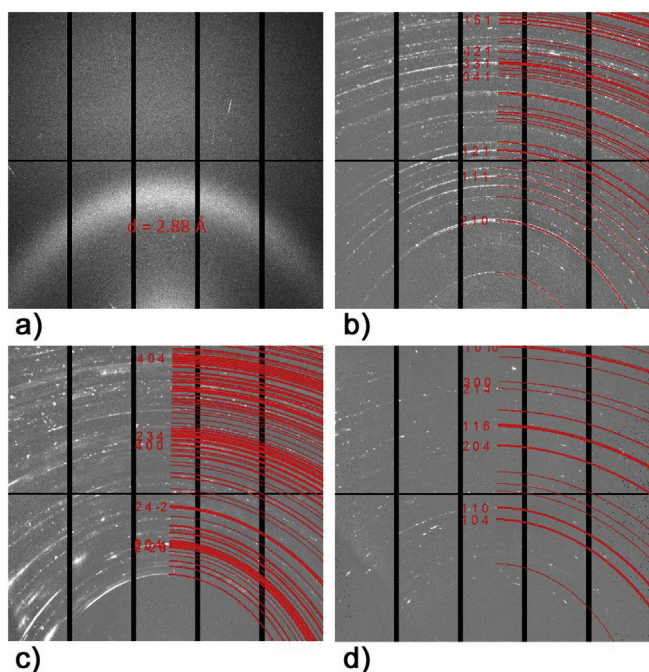


**Fig. 5.** Synchrotron X-ray microdiffraction images of Motoujina fallout debris for phase identification (some Debye rings are indexed). (a) Glassy filament shows an amorphous phase; (b) Microcrystalline area dominated by mullite; (c) Microcrystals indexed as anorthite; (d) A Fe-rich area with dendrites showing mostly hematite.

### 3. Results

#### 3.1. Sandstone petrography and Motoujina fallout debris abundance

The Motoujina beach sands comprise coarse- to very coarse-grained, moderately sorted weathering products derived from the Cretaceous-age granites, which constitute much of the bedrock of the Hiroshima Bay (Fig. S2; [Geological Survey of Japan, 1985](#)). Sandstone petrography reveals the bulk of the natural sediments to comprise angular to sub-angular, translucent quartz, milky feldspar grains, with subordinate biotite crystals and rare slate and arenite debris. The MFD stand out as generally shiny, rounded glasses, easily distinguishable from the angular grains of the host sediment.

For each Wentworth granulometric class, we combined and scale-up the estimated number of examined grains and the number of recovered MFD to derive an average percentage of MFD per sediment grains ([Table 1](#)). Assuming a linear relationship between the weight of the dry sample and the average percentage of MFD present in each grain size class, we derived an average

**Table 1**  
Combined grain counts distribution per granulometric classes and average percentage of Motoujina fallout debris (based on [Tables S4 & S5](#)).

Wentworth granulometric classes	Estimated total number of sediment grains examined	Number of recovered MFD	Average % of MFD per sediment grains
Fine Granules	3,700	23	0.6
Very coarse sand	63,300	799	1.3
Coarse sand	1,17,800	2,906	2.5
Medium Sand	1,86,400	3,691	2.0
Fine sand	1,19,600	1,865	1.6
Very fine sand	27,600	232	0.8
Silt and Clay	8,400	79	0.9

concentration of nearly 18 g of MFD per kilogram of dry sand. Assuming an uncertainty range of plus/minus 30%, the concentration of MFD may be as low as 12.6 g or as high as 23.3 g per kilogram of dry sand ([Table 2](#); [Supplementary Text \(a\) & Table S3](#)), where nearly 75% of the MFD mass consists of coarse to very coarse sand-size particles. The highest recorded concentration of MFD is in coarse sands, where the fraction of fallout debris represents 2.5% of all grains. For comparison, the lowest concentration of MFD is recorded within fine granules, where it represents 0.6% of all grains.

#### 3.2. Motoujina fallout debris morphological groups

Overall, MFD are aerodynamically-shaped and characterized by a highly diverse morphology, texture and composition. They can be divided into six different morphological groups according to the set of criteria listed in [Table 3](#).

Group 1 comprises shiny glasses and includes larger-size, volumetrically dominant (43.2%) vesicular glass fragments ([Figs. 2A & S3](#)), crystal clear, bubble-free glass spherules as well as spherules with abundant gas bubbles, tainted and with inclusions ([Figs. 2B, C & S4](#)) and vesicular glass filaments ([Figs. 2D, E & S5](#)); nearly two thirds (61.9%) of all MFD consist of Group 1 debris. Group 2 consists of opaque, aerodynamically-shaped debris often fused and covered by a thin coat of translucent glass melt ([Figs. 2F, H, M & S6](#)). Opaque, silica-covered, spheroid and fused debris of varying composition ([Figs. 2I–L, S7 & S8](#)) are categorized in Group 3. Group 4 includes debris of meta-sediments (mostly slates) coated with amorphous glass and occasionally fused with glass and other debris ([Fig. 2N, O & S9](#)). One fourth (25.3%) of all MFD consist of debris from Groups 2, 3 and 4. Group 5 includes a less well-understood type of MFD that superficially look like metallic particles but appears to be of rubber-like composition ([Fig. S10](#)); about one-tenth (10.7%) of all MFD are Group 5-type debris. Other miscellaneous melt debris including obsidian- and pumice-like debris ([Fig. S11](#)) are included in Group 6, a volumetrically minor group (2.1%).

Based on optical microscopic observations, glass melts often show successive episodes of concentric coating (e.g. [Figs. S7F–7L; S9F, I, J, M, S–X](#)); this may reveal a complex suite of cooling steps within an over-heated environment. The morphology of the successive silica concentric coats from thin to thick suggests an increase in viscosity towards the younger, outermost layers. By analogy, trinitite glasses include high-Si and low-Si glasses which differ by several orders of magnitude in viscosity and indicate minimal mixing ([Eby et al., 2015](#)).

#### 3.3. Motoujina fallout debris microstructures, chemical compositions and mineralogy

Backscatter images illustrate a clear glass sphere ([Fig. 3a](#)), a clear glass filament ([Fig. 3b](#)), a more complex particle with melt structures and droplets of a Fe-Cr alloy (white in [Fig. 3c](#)). Colored particles display complexities, such as dendritic growth structures of iron oxides ([Fig. 3d](#)), flow structures resembling volcanic rocks with Fe-rich crystallites ([Fig. 3e](#)) and particles with Al-Si-Ca rich crystallites ([Fig. 3f](#)). The chemical composition was estimated from EDS X-ray spectra ([Fig. 4](#)): clear particles is a glass composed of CaO (43 weight %), SiO<sub>2</sub> (33%), Al<sub>2</sub>O<sub>3</sub> (15%) and MgO (7%), with a significant amount of sulfur (1.5% SO<sub>3</sub>; [Fig. 4a](#)). Based on SEM-EDS analyses ([Fig. 4d](#)), rubber-like particles ([Fig. S10](#)) consist mainly of carbon and oxygen, with some sulfur and include nanocrystalline pockets richer in Si, Al, K and Ca, probably derivatives from glass ([Fig. 4d](#)).

[Fig. 5](#) displays micro-x-ray diffraction images and [Fig. S12](#) the corresponding integrated diffraction spectra. The glassy spherules

**Table 2**

Estimates of the mass of Motoujina fallout debris in different granulometric classes for one kilogram of dry beach sand, Motoujina Peninsula.

Wentworth granulometric classes	Dry sediment fraction weight (g) normalized for 1 kg	Average % of MFD per sediment grains	Estimated mass of MFD (g/kg) per grain-size class	MFD weight % by grainsize class
Fine Granules	108.59	0.6	0.7	3.9
Very coarse sand	289.36	1.3	3.8	21.1
Coarse sand	378.20	2.5	9.3	52.1
Medium Sand	154.67	2.0	3.1	17.1
Fine sand	66.25	1.6	1.1	5.9
Very fine sand	2.94	0.8	0.0	0.1
Silt and Clay	0.01	0.9	0.0	0.0
<b>Estimated mass of MFD in 1 kg dry sand (g/kg)</b>			<b>17.9</b>	
<b>Low estimate:</b>		<b>Minus 30%</b>	<b>12.6</b>	
<b>High estimate:</b>		<b>Plus 30%</b>	<b>23.3</b>	<b>73.2</b>

and filaments were confirmed as amorphous with a diffuse diffraction ring at 2.88 Å (Fig. 5a, corresponding to specimen on Fig. 3b). More complex microcrystalline particles (Fig. 3f) in a glass matrix were found to consist of mullite and anorthite (Fig. 5b, c), while Fe-rich dendrites (Fig. 3d, e) were identified as hematite (Fig. 5d; see also Fig. S12). Magnetite may also be present but has only been documented by magnet tests.

#### 4. Discussion

##### 4.1. Preservation of Motoujina fallout debris

The low tidal range (<2 m) and the weak "principal lunar semi-diurnal" (M2) tidal currents (<30 cm/s in Takeoka, 2002), combined with the lack of strong waves in the Seto Inland Sea, create a low-energy environment where the sediments experience no significant hydraulic winnowing, maintaining a poorly sorted grain size distribution (Fig. S2) and limiting the general abrasion or physical/chemical weathering of the sand grains. In addition, studies of the tidal flow around the nearly closed Hiroshima Bay (Zhang et al., 2003) indicate that the exchange ability of the water

in it is weak, resulting in poor evacuation to the open sea. Such a protected environment explains the preservation of delicate glass debris within moderately sorted and mostly angular siliceous sand grains (e.g., Fig. 2G). The air-fall particles represent an addition of unique foreign particles to a local siliceous sediment population, with genuinely robust subsequent preservation and minimal reworking in a sandy, but fairly low energy environment.

##### 4.2. Estimated Motoujina fallout debris mass

Based on the estimate that 1 kg of dry sand includes on average nearly 18 g of MFD (Table 2), assuming a homogeneous distribution of this percentage and that one cubic meter of dry sand weighs 1530 kg (Supplementary Text (b)), the total mass of MDF within the upper 10 cm of the Motoujina beaches may be in the order of 36 metric tons (Table S6). For a low estimate of 12.6 g of MFD per kilogram of dry sand, based on a notional 30% cut of the average estimate, the Motoujina beaches may still hold nearly 25 metric tons of MFD.

As no physical basis allows for restriction of MFD to the beach sands of Motoujina and given the occurrence of fallout debris on

**Table 3**

Motoujina fallout debris groups and descriptions with abundance and relative percentage (Groups 2, 3 and 4 were not differentiated during the initial analysis).

MFD groups	Diagnostic criteria	Description	Figures	Number of counted debris	Group %
Group 1	Glass fragments, shiny, vesicular	Single sub-rounded and distinctly vesicular debris, shiny, translucent or tinted, occasionally with opaque domains; non-coated, non-magnetic, occasionally with inclusion of angular microdebris; larger specimens can be over 2 mm in size	S3	4142	43.2
	Glass spherules, generally shiny	Single spheres or fused with smaller spherules, shiny, translucent, tinted or opaque, sometimes black; occasionally with secondary surface coat; occasionally vesicular; non- to weakly magnetic	S4	1214	12.7
	Glass filaments, shiny, vesicular	Single, thin and elongated debris, translucent, occasionally with attached glass drops or fused together, non-coated, non-magnetic debris	S5	580	6.0
Group 2	Opaque, dull, aerodynamically-shaped debris	Single and complex fused spheroids, opaque, non-shiny, occasionally with translucent silica layers; non- to weakly magnetic	S6	2426	25.3
Group 3	Silica-coated, opaque, aerodynamically-shaped debris	Fused aerodynamically-shaped, rounded debris, opaque, partially to fully coated with one or various silica layers; individual debris may include Group 1, 2, 4 and/or 6 type debris; non- to weakly magnetic	S7		
	Silica-coated, opaque, flattened debris	Flattened, sub-angular and irregular-shaped opaque debris, partially to fully coated with one or various silica layers; individual debris may include Group 1, 2, 4 and/or 6 type debris; non- to weakly magnetic	S8		
Group 4	Meta-sediments with blobs of opaque silica glass Meta-sediments incorporated in complex fallout debris	Single, rounded to sub-rounded fragments of fine-grained or crystalline metasediments, partially overlain with blobs of opaque silica melts; non-magnetic Fused, aerodynamically-shaped opaque debris incorporating metasediments, often with later superficial silica coating; non- to weakly magnetic	S9		
Group 5	Rubber-like, opaque debris with complex surface texture	Single, rounded to sub-angular, opaque debris with a smooth to highly sculpted surface; occasionally incorporate angular micro-debris	S10	1028	10.7
Group 6	Miscellaneous MFD	Miscellaneous opaque, composite, aerodynamically-shaped debris with e.g. pumice-like and obsidian-like composition	S11	205	2.1

the shores of nearby Miyajima Island, it is likely that MFD are also present in shelf sands in the vicinity of Motoujina Peninsula. Based on the same assumptions, one square kilometer of shelf sands (Fig. S13) down to a depth of 10 cm may hold on average over 2800 metric tons of MFD; a low estimate would still account for nearly 2000 metric tons of MFD (Table S6).

The accumulation of such large volumes of melt debris as estimated above requires a massive catastrophic event to have occurred recently and in close proximity.

#### 4.3. Conditions of Motoujina fallout debris formation

Because aerodynamically-shaped glasses, including spherules, indicate a high-velocity, high-temperature genesis, the presence of these particles within the beach sands is thought to result from an aerial fallout. Superficial glass coating is found on nearly all types of aerially-generated melt particles: silica coating is observed on vesicular glass debris (Figs. S11A & B), on spherules (Fig. S7A), on opaque, aerodynamically-shaped debris (Fig. S6), on a variety of complex, amalgamated debris (Fig. S6) as well as on meta-sediments (Figs. S9A–G). Such coatings have not been observed on glass filaments nor on rubber-like debris, but it cannot be excluded that such debris are present under the opaque coat of some amalgamated debris. This feature shared by most groups of MFD indicates a co-genetic origin and points to a single generating event. Silica-coatings are absent on quartz and feldspar grains that form the bulk of the natural beach sand.

The dominant Ca-rich composition of MFD glasses does not match the chemical composition of felsic granites such as those present in the Hiroshima Bay and therefore indicates that the bulk of the volatilized materials at the origin of the MFD is unrelated to the local bedrock. On the phase diagram of the CaO–Al<sub>2</sub>O<sub>3</sub>–SiO<sub>2</sub> system (Fig. 6), the composition of clear glasses indicates a formation temperature above 1400 °C.

The presence in MDF of a mullite-anorthite assemblage is diagnostic for a unique genesis as no natural assemblage of these two phases has yet been encountered. The anorthite solidus in the system CaO–Al<sub>2</sub>O<sub>3</sub>–SiO<sub>2</sub> exceeds a temperature of 1500 °C (Fig. 6,

e.g., Mao et al., 2006). At ambient pressure, the silica-mullite solidus temperature is 1595 °C and the alumina-mullite solidus temperature is 1840 °C (Risbud and Pask, 1978). Therefore, it appears likely that the temperature of the melted and vaporized materials that quenched into MFD may have been in the order of 1800 °C–2000 °C.

Iron enters into the composition of many MFD particles: hematite dendrites are dominant among the iron-rich particles (Fig. 3d) and we have also observed native iron globules (Fig. 3c). This suggests a wide range of oxygen fugacities (>5 orders of magnitude) as displayed in the fO<sub>2</sub>-T phase diagram (Fig. S14). The presence of magnetite has not been confirmed but is likely present in some MFDs based on the magnetic signatures. Such a range of fugacities is to be expected during a turbulent environment in the atmosphere with large local temperature gradients.

MFD have been recovered from the beach sands to a depth of about 10 cm, where the youngest, “modern” beach sands have been deposited. Though these dominantly coarse-grained sands are subjected to diurnal tidal cycles, the preservation of delicate glass filaments (Figs. 2E, S5) and the absence of abrasion on most of the MFD denotes a short residence time at geological time scales, i.e. their origin is likely a relatively recent event. Although conventional radiometric dating techniques are currently unavailable to date glasses of a very recent to historical age, the presence of selected short-lived radionuclides produced in nuclear detonations could be used to limit the age of the MFDs. If confirmed, the presence of rubbery fallout particles would indicate a young, Holocene age for the origin of the MFD.

This study suggests that a recent, single and massive catastrophic event that involved temperatures in excess of 1800 °C led to the formation of the fallout debris encountered in Hiroshima Bay.

#### 4.4. Potential natural origins of fallout debris

Micrometeorites are micrometer to millimeter size debris from comets and asteroids that entered the Earth system through gravity; while passing through the atmosphere, some of these debris were melted and quenched into glass spherules, whereas others retained their original mineral composition. Micrometeorites have diagnostic characteristics in their chemical composition, reflecting their chondritic or achondritic origin (e.g., Koeberl and Hagen, 1989, cite olivine and over 30 constituent trace elements, including iridium). Similar to some MFD found in this study, cosmic spherules have a shiny and smooth dark surface (Koeberl and Hagen, 1989) and are magnetic. Cosmic spherules with welded microspherules (Figure 7D in Kyte, 2002), complex spheroids (Figure 7E in Kyte, 2002) and glass spherules with an attached filament tail (Fig. 5 in Taylor et al., 2000) are morphotypes also encountered in MFD.

Cosmic spherules are unstable under normal Earth conditions and are prone to weather rapidly unless collected shortly after their landing or preserved under special circumstances. Recently, however, Genge et al. (2017) provided evidence for their presence in some urban environments, when collected immediately following deposition.

We note that the chemical composition of MFD differs from that of cosmic spherules and that there is no indication for the presence of olivine (and no significant amounts of Mg). The MFD display an unusual morphological diversity and are present in significant concentration in coarse angular sands. As a result, and considering their apparent limited geographical distribution, we conclude that the single event at the origin of MFD is unrelated to particulate cosmic rain.

Fallout debris from cosmic airbursts, i.e., the explosive breakdown of a cometary or asteroid body in the atmosphere,

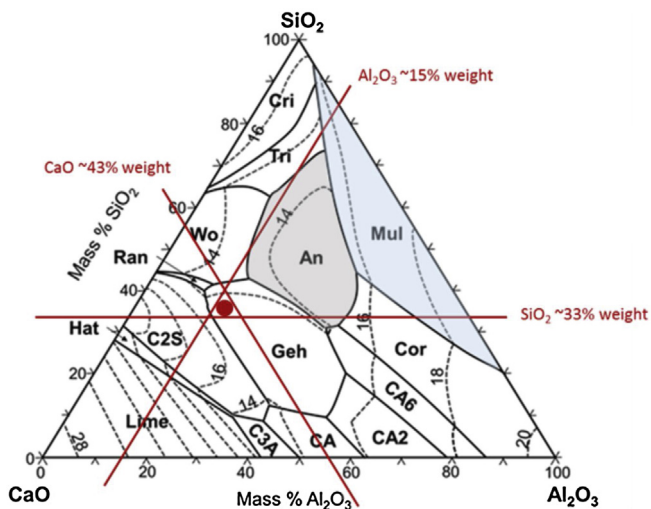


**Fig. 6.** Phase diagram of the calcium oxide-aluminium oxide-silicon oxide (CaO–Al<sub>2</sub>O<sub>3</sub>–SiO<sub>2</sub>) system (from Mao et al., 2006). The red dot shows clear glass particles composition from Fig. 4 and indicate a solidus above 1400 °C. The dashed curves represent the isothermal sections and the numbers stand for the temperatures with the unit as hundred Celsius. An, anorthite (grey field); CA (CaO•Al<sub>2</sub>O<sub>3</sub>); CA2 (CaO•2 Al<sub>2</sub>O<sub>3</sub>); CA6 (CaO•6Al<sub>2</sub>O<sub>3</sub>); C3A (3CaO•Al<sub>2</sub>O<sub>3</sub>); C2S (Ca<sub>2</sub>SiO<sub>4</sub>); Cor, corundum; Cri, cristobalite; Geh, gehlenite; Hat, Hatrurite; Mul, mullite (blue field); Wo, wollastonite; Ran, rankinite; Tri, tridymite.

constitute a class of debris not well understood (Wasson, 2003). Though unrelated in age and in aerial distribution, the descriptions of silica- and iron-rich microspherules, of vesicular, high-temperature, siliceous scoria-like objects, including the presence of mullite all compare well with MFD (Bunch et al., 2012; Wittke et al., 2013). The mechanism of a cosmic airburst remains controversial and would not apply in the case of MFD, as no supra-regional areal spread of fallout debris can be demonstrated.

*Microkrystites* and *microtektites* comprise sand-size crystal and glass fallout spherules created when large extraterrestrial objects strike the Earth at cosmic velocity and eject liquefied or volatilized ground materials from the crater into the atmosphere (Glass and Simonson, 2013). The composition of microlites and crystallites in microkrystites usually reflects the chemistry of both the vaporized projectile and the target rock (Glass and Simonson, 2013). Microtektites and the larger, gravel-size tektites are a subgroup of impact glasses, the chemistry of which generally reflect the composition of the impact target rocks (e.g., Blum et al., 1992; Koeberl, 2014). Their presence defines four major strewn fields on Earth, none of which extends to the Japanese archipelago. We also note that the composition and diversity of MFD do not match those of microtektites.

Lightning during volcanic eruptions can generate glass spherules, which are found associated with abundant ash deposition (Genareau et al., 2015). The region of Hiroshima is one of the least exposed to volcanic activity in Japan and there is no known historic record of volcanic ash-fall on the city. The nearest volcanoes have all been dormant in historical time; within a radius of 80 km around the city, they include the Sanbe stratovolcano and the Abu Shield Volcano Group. Mount Aso, a large, active stratovolcano is located about 200 km SW of Hiroshima. A possibility for MFD spherules to have originated through extrusive processes can be discarded, more so that it would not explain the origin of the other types of fallout debris. The morphology of Pele's tears approaches that of some MFD filaments (Porritt et al., 2012), but these volcanic pyroclasts are found associated with basaltic explosive eruptions which have not been observed in the vicinity of Hiroshima.

We conclude that naturally occurring fallouts cannot serve as a viable source for the melt particles observed at Motoujina. Though their morphology in-part overlaps with that of glasses formed through natural phenomena, the high concentration/high diversity of melts at Hiroshima Bay and the unique nature of the vesicular glass shards, the vesicular filaments, the composite glazed debris and the rubber-like components, coupled with the absence of an identified strewn field all indicate that one must find an alternative explanation for their origin.

#### 4.5. Potential anthropogenic origin of fallout debris

Three main scenarios can explain the presence of melt particles resulting from human activity in the Motoujina samples: (1) fallout debris originating from fireworks, (2) from industrial contaminants and (3) from the Hiroshima A-bomb detonated on August 6th, 1945.

The Hiroshima Port Dream Fireworks Festival is held in July every year and during the event as much of 10,000 fireworks are set off in the bay, about 1 km to the East of Motoujina (Fig. 1). The high heat generated during the aerial explosion of fireworks can lead to the formation of spherules. Grima et al. (2011) have described these fallouts as having generally a regular spheroidal shape, although some particles may be hollow-shaped. All these particles are very small, varying in size within the range of 0.5–5 microns. The chemical composition of these microspherules can show large variations depending on the original mixture of the firework. However, there is a lack of knowledge about this type of

fallouts and data on their morphological characteristics, their chemical composition, and their abundance do not exist.

In order to compare firework-generated fallout particles with the Motoujina melts, we have sampled the Kuala Lumpur City Centre (KLCC) Suria esplanade in front of the Petronas towers in the morning of January 1st, 2017, a few hours after the massive end-of-year display of fireworks. Dust was sampled, and particles were captured with magnets, which we assume are fallouts from the overhead firework. Over one hundred aerodynamically shaped metallic particles were collected; most of them are smaller than 50  $\mu\text{m}$ , yet systematically larger than the particles described by Grima et al. (2011).

The larger fallout particles sampled at KLCC (Fig. S15) are large metallic spherules, 0.7 mm in diameter, and complex spheroids including fused smaller spherules. Whereas the morphology of these fallouts overlaps with MFD (compare Figs. S15A and S6A), the composition of firework-generated fallout particles appears to be limited to metallic, subordinate glass spherules and spheroid bodies. KLCC spherules are near-vertical fallouts in comparison with firework-generated spherules in Motoujina that would have to be derived from 1 km away. Whereas it cannot be excluded that some of the smaller spherules found in Motoujina are derived from the fireworks in the Hiroshima Bay, the origin for the majority of MFD (vesicular glass shards and filaments and ground debris with melt products) is definitely unrelated to fireworks.

In December 2004, a fire occurred at the paint shop of the Mazda Ujina No. 1 Plant at Hiroshima Bay, about three kilometers NW of the Motoujina Peninsula (Fig. 1); the fire started at around 23:00 and lasted for approximately 7 h before it was extinguished. Painting robots, pipes, and air-conditioning equipment were damaged in the fire but apparently “none of the paints or other materials used in the painting line contains heavy metals or other hazardous substances” (Mazda Motor Corp, 2005). From the limited data released by Mazda, it is likely that much of the materials released into the atmosphere during the fire consisted of plastic and asphalt-bearing products. Aerial transportation in the range of one kilometer was limited to the less dense cloud and most likely only involved micron-size particles. Some minute plastic debris may have reached Motoujina, but this fire cannot serve as a source for the glass-dominated MFD.

Fly-ash, steel slags and glassy spherules of industrial origin (e.g., Marini and Raukas, 2009; French and Koeberl, 2010) are other potential anthropogenic microtektite-like contaminants. While such elements may be present within the MFD population, the diversity of particles found at Motoujina is significantly larger and includes debris such as glass filaments and coated debris, the origin of which is not known from industrial contamination.

#### 4.6. Nuclear fallout debris and the atomic explosion at Hiroshima City

No studies have described the material fallout debris resulting from nuclear explosions at either Hiroshima or Nagasaki, the only two urban areas where atomic bombs have detonated. In the days following the Hiroshima explosion, a team of scientists from the Institute of Physical and Chemical Research led by Yoshio Nishina collected sands and other specimens from 28 locations in the city. At the same time, scientists from the Kyoto Imperial University took soil samples during two sampling trips to Hiroshima (Hiroshima Peace Memorial Museum). All these samples were analyzed for radioactivity and apparently no attention was given to a physical description of the samples (Imanaka, 2011b).

Over 2053 nuclear weapons tests were carried out from 1945 to 1998, of which over 500 have been nuclear atmospheric tests carried out prior to 1963 (Waters et al., 2015). All these tests were conducted in natural and non-urban, remote sites. Despite this large number of tests and the observation that nuclear explosions



generate large volumes of glass materials (e.g., Pacold et al., 2016), description of nuclear fallout debris is limited to a few vintage publications (e.g., Adams et al., 1959; Miller, 1964), de-classified studies from USA test sites and recent nuclear forensic studies (e.g., Eppich et al., 2014; Weisz et al., 2017).

Researchers have analyzed in great detail the fused glasses lining the Trinity crater at the site of the first nuclear test at Alamogordo (New Mexico), on July 16, 1945 (e.g. Hermes and Strickfaden, 2005; Eby et al., 2010). Originally it was assumed that these glasses named “trinitite” were formed on the ground. However, in a new study, Eby et al. (2015) argued that most of the trinity glass was deposited as “trinitite rain”. Individual fallouts from nuclear tests have been the subject of petrographic descriptions, chemical composition studies and radioactivity measurements (Adams et al., 1959; Miller, 1964). Described fallout debris include glass beads and spherules up to 500 µm in diameter, often weakly magnetic, vesicular and with fused smaller spherules; other debris include black, magnetite spherules and spheroidal particles or agglomerates (Adams and O’Connor, 1957; Miller, 1964). Some fallouts from surface shots and shallow underground detonations in Pacific atolls are fused on ground debris (Miller, 1964).

Within the last decade, research programs into nuclear forensics post-detonation analysis have resulted in a large number of publications describing the elemental and isotopic composition of trinitite and fallout glasses (e.g. Eppich et al., 2014) and complex-shaped, agglomerated glasses (Weisz et al., 2017). The analyses are restricted to selected specimens and no data are shared on the diversity and amount of fallout debris generated by the explosions. There is no account from nuclear test sites of vesicular glass shards, glazed composite debris and other types of debris encountered in Motoujina. At least, no direct analog is available from open source literature.

An aerial nuclear explosion over an urban area would volatilize a higher diversity of materials as compared to an explosion over a desert or an atoll and it can be expected that such fallouts would reflect this initial compositional heterogeneity. Detailed reports are available about the fateful event that erased the city of Hiroshima on August 6th, 1945 (US Strategic Bombing Survey, 1946). “Little Boy”, the 4,400-kilogram atomic device dropped by the B-29 Superfortress Enola Gay contained about 64 kg of enriched Uranium-235; it detonated at 08:15 am, at an air burst height of  $600 \pm 20$  m above ground (Kerr et al., 2005). The blast yield is estimated at  $16 \pm 2$  kilotons TNT; the core of the fireball reached extremely high temperature ( $> 10^7$  K) and pressure ( $> 100$  GPa); the front of the shock wave reached the ground after one second, whereas the fireball ascended without touching the ground; no crater was formed (Imanaka, 2011a). The expanding shock wave massively devastated the city within a radius of 3600 m. Driven by strong updraft winds, heterogeneous ground materials from the urban environment charged the rapidly inflating atomic cloud. Within about 3 min the atomic cloud reached a height of 8 km, ascending further to a height of 15 km after 15 min (Baba et al., 2011; Fig. S16). Huge firestorms engulfed the city and fed the base of the cloud, spreading laterally 1–3 kilometers above ground. This basal cloud was laden with soot from the fires and delivered the radioactive “black rain” (Ohtaki, 2011).

Following the nuclear explosions at both Hiroshima and shortly after at Nagasaki, and the devastation at a scale not seen before, the rescuers, doctors, and scientists focused their efforts on curing human suffering and measuring the effects of atomic radiation. Technical teams from the US (U.S. Strategic Bombing Survey, 1946) and from Great Britain (British Mission to Japan, 1946) assessed in great details the level of physical devastation of these two cities, in order to measure the destructive capabilities of nuclear bombs. Somehow, in this situation of extreme emergency, the question of

the whereabouts of the vanished urban built structures was not addressed.

#### 4.7. Diagnostic criteria linking Motoujina fallout debris with the Hiroshima A-bomb explosion

Because of close proximity with the A-bomb’s hypocenter, the presence of a rich and diverse association of aerially-generated melt fallout debris around the Motoujina peninsula in Hiroshima Bay inevitably suggests a link with the August 6th, 1945 nuclear explosion. These debris are present in all 13 analyzed Motoujina surface beach samples at locations 6 km south of the bomb hypocenter. Four beach sand samples from Miyajima Island, 12 km away from the hypocenter (Fig. 1) also include melt debris, though generally smaller in size, in significantly lower concentration and lower diversity.

At Motoujina, the well-preserved association of melt fallout debris including fragile, aerodynamically-shaped glasses in coarse to very coarse beach sands points to a recent depositional event within the modern sediments. The association of abundant vesicular glass debris, vesicular glass filaments and complex agglomerates of diverse melt particles and ground debris coated with up to three successive superposed films of amorphous glass have not been described from other nuclear test sites. Multiple successive glass coatings encountered on MFD indicate a relatively long residence time within a complex high-temperature aerial environment compatible with that of an atomic cloud. As this secondary silica coating is present on most groups of MFD, its origin is most likely the result of a single formational event.

Assuming only a 500-meter radius area around the hypocenter, Imanaka (2011a) estimated at 15,000 tons the amount of dust created by the Hiroshima A-bomb blast. We evaluate the volume of the atomic cloud after 3 and 15 min at respectively 60 cubic kilometers and nearly 675 cubic kilometers and its mass to be on the order of several hundred thousand tons (SI: Supplementary Text (b); Fig. S16). In our estimation, the firestorm that devastated over 10 square kilometers of the city required a mass of combustible materials exceeding 300,000 tons (Glasstone and Dolan, 1977; SI: Supplementary Text (c); Fig. S17).

We estimate the mass of MFD potentially present in shelf sands over an area of one square kilometer to be in the order of two to three thousand metric tons (Table S6); this represents less than one percent of the materials destroyed by the A-bomb. The mass estimates of destructed urban material and the mass of MFD present over a fraction of the ground below the atomic cloud appear to have matching orders of magnitude, which strengthen the hypothesis of a cause-and-effect relationship between the A-bomb and the MFD.

The MFD chemical composition differs from that of the felsic granitic rocks forming the bedrock of the Hiroshima Bay. The dominant Ca-rich composition of MFD glasses possibly originated from concrete (Sawaki et al., 2009), especially if limestone or marble was involved in its mix. Also, bricks and roof-tiles (Si-Al) would fit that pattern. Fe-Cr droplets in the fallouts and precipitates of hematite have likely originated from steel.

The presence of mullite nanocrystals embedded in MDF suggests a formation temperature in excess of 1800 °C for these aerodynamically-shaped debris. The joint presence of mullite and anorthite nanocrystals appear to be a unique occurrence, consistent with an anthropogenic origin. No naturally occurring mullite-anorthite assemblages have been described, although they are important in high-temperature ceramics (Miao et al., 2014), including ceramics produced from urban waste (Hua et al., 2016).

Initial attempts to determine if low-background radioactivity could be detected in MFD have been carried out deep underground at the Grand Sasso laboratory in Italy (C. Koeberl, pers. communication); these studies have so far been inconclusive.

This may appear surprising since glasses from ground Zero at the Trinity test-site retain some radioactivity. However, in this case of the fireball interacting with the ground, CaMgFe glasses sequester all radioactivity (Williamson et al., 2016). In comparison, the fireball resulting from the high-altitude explosion at Hiroshima did not touch the ground (Imanaka, 2011a) and MFD are relatively distal fallouts from the atomic cloud. It is not yet established if CaMgFe glasses or even lechatelierite are present in MFD. Further investigations of remaining radioactivity at the submicroscopic scale would be appropriate, using similar technology as applied by Eby et al. (2010) for trinitite.

## 5. Conclusions

This study has revealed the presence of unique types of melt debris of high velocity and high-temperature origin ( $>1800^{\circ}\text{C}$ ), in high concentration (thousands of metric tons per square kilometer), only a few kilometers away from the Hiroshima A-bomb hypocenter in Japan. We conclude that there is a preponderance of supporting evidence for their origin to be linked to the nuclear explosion of August 6th, 1945. We acknowledge that selected Motoujina fallout debris are analogous to some impact glasses and that a variety of firework- and industrial-derived melt debris cannot be distinguished from some MFD; yet no alternative scenario to the A-bomb explosion can provide a coherent explanation for all our observations.

The preservation of delicate glass filaments and the overall pristine condition of MFD within modern, coarse-grained beach sands at Motoujina indicate a recent depositional event and the presence of rubber-like debris within MFD points to a recent age. The large volume of MFD likely present within the Hiroshima Bay sands, their aerodynamic shape, the inclusion of very high-temperature nanocrystals and their shared, single origin all indicate that a unique, massive explosion at close proximity led to their formation.

The MFD differ in a number of ways from fallout debris described from other, near-ground nuclear explosions. First of all, their mass is dominated by vesicular glass debris, a type of fallout not reported from test sites and different from fused trinitite glasses which were formed by the fireball in the immediate vicinity of ground zero (e.g., Eby et al., 2015). Elongated glass filaments are another type of fallout debris unknown from test sites. Multiple glass coats on amalgamated fallout debris also appear to be a unique feature of MFD. All these distinctive features separate “Hiroshimaites” from other types of fallout debris.

This study is the first to describe these unique fallout debris. It sets the foundations for future, more quantitative assessments of their geographic distribution and chemical composition. The identification of microcrystalline phases that are present will provide further constraints about their cooling histories. The composition of rock fragments associated with MFD, the microdebris inclusions in glass particles, microstructures and local inhomogeneities will clarify the origin and degrees of metamorphism of ground debris. Confirmation of the rubber nature of a group of MFD will demonstrate their recent, anthropogenic origin. The search for clues linking the composition of MFD to original constituent materials of the urban environment would open the way for an entirely new area of research. Additional studies should look at their radionuclide compositions and eventual residual radiation. Further investigations of remaining radioactivity at the submicroscopic scale would be appropriate, using similar technology as applied by Eby et al. (2010) for trinitite. The search for similar aerodynamically-shaped glasses and melt debris at other locations in the Hiroshima and Nagasaki area will further diagnostically constrain our hypothesis linking MFD/Hiroshimaites

formation to the August 1945 A-bomb explosion. Ultimately, further studies and models should advance our understanding of such explosions and their long-term (decadal to centurial) environmental effects.

## Declarations of interest

None.

## Acknowledgments

For their thorough review of the draft manuscript and suggestions for improvements, we are indebted to Ricardo N. Alonso (UNSA-CONICET, Salta, R. Argentina), Steven Bergman (gentleman geologist living on Vashon Island in the Puget Sound, WA, formerly Shell R&D Houston), Isabelle Coutand (Dalhousie University, Halifax), Fred Keller (formerly Shell Exploration, Houston), Christian Koeberl (Universität Wien), Martin Kunz (University of California, Berkeley), Bradford E. Prather (University of Kansas, Lawrence) and an anonymous reviewer. Dr. Siang Leng Goh (Singapore) provided samples from Miyajima Island and Satoko Suzuki (Yakuin, Chuo-ku, Fukuoka-shi, Fukuoka) helped with logistical matters. We also appreciate comments by editors of *Anthropocene*, Nelson Eby (University of Massachusetts, Lowell) and an anonymous reviewer that helped to improve the manuscript.

HRW is appreciative for support from NSF (EAR 1343908) and DOE (DE-FG02-05ER15637). We acknowledged access to beamline 12.3.2 of the Advanced Light Source, which is a DOE Office of Science User Facility under contract no. DE-AC02-05CH11231, and the Zeiss EVO SEM at EPS, UC Berkeley. Tim Teague helped with sample preparation and SEM analyses.

## Appendix A. Supplementary data

Supplementary material related to this article can be found, in the online version, at doi:<https://doi.org/10.1016/j.ancene.2019.100196>.

## References

- Adams, C.E., O'Connor, J.D., 1957. The Nature of Individual Radioactive Particles. VI. Fallout Particles From A Tower Shot, Operation Redwing. Research and Development Technical Report USNRDL-TR-208. Classified document with available abstract.
- Adams, C.E., Farlow, N.H., Schell, W.R., 1959. The composition, structures and origins of radioactive fall-out particles. *Geochim. Cosmochim. Acta* 18, 42–56.
- Baba, M., Ogawa, F., Hiura, S., Asada, N., 2011. Height estimation of Hiroshima a-bomb mushroom cloud from photos. In: Aoyama, M., Oochi, Y. (Eds.), *Revisit the Hiroshima A-Bomb with a Database: Latest Scientific View on Local Fallout and Black Rain*, pp. 55–67.
- Blum, J.D., Papanastassiou, D.A., Koeberl, C., Wasserburg, G.J., 1992. Nd and Sr isotopic study of Australasian tektites: new constraints on the provenance and age of target materials. *Geochem. et Cosmochim. Acta* 56, 483–492.
- British Mission to Japan, 1946. The Effects of the Atomic Bombs at Hiroshima and Nagasaki. His Majesty's Stationary Office, London 21pp.
- Bunch, T.E., Hermes, R.E., Moore, A.M., Kennett, D.J., Weaver, J.C., Wittke, J.H., DeCarli, P.S., Bischoff, J.L., Hillman, G.C., Howard, G.A., Kimbel, D.R., 2012. Very high-temperature impact melt products as evidence for cosmic airbursts and impacts 12,900 years ago. *Proc. Natl. Acad. Sci. U. S. A.* 109 (28), E1903–E1912.
- Eby, N.G., Hermes, R., Charnley, N., Smoliga, J.A., 2010. Trinitite—the atomic rock. *Geol. Today* 26 (5), 180–185.
- Eby, N.G., Charnley, N., Pirrie, D., Hermes, R., Smoliga, J., Rollinson, G., 2015. Trinitite redux: mineralogy and petrology. *Am. Mineral.* 100, 427–441.
- Eppich, G.R., Knight, K.B., Jacomb-Hood, T., Spriggs, G.D., Hutcheon, I.D., 2014. Constraints on fallout glass formation from a near-surface nuclear test. *J. Radioanal. Nucl. Chem.* 302, 593–609.
- French, B.M., Koeberl, C., 2010. The convincing identification of terrestrial meteorite impact structures: what works, what doesn't, and why. *Earth. Rev.* 98, 123–170.
- Genareau, K., Wardman, J.B., Wilson, T.M., McNutt, S.R., Izbekov, P., 2015. Lightning-induced volcanic spherules. *Geology* 43 (4), 319–322.
- Genge, M.J., Larsen, J., Van Ginneken, M., Suttle, M.D., 2017. An urban collection of modern-day large micrometeorites: evidence for variations in the extraterrestrial dust flux through the quaternary. *Geology* 45 (2), 119–122. doi: <http://dx.doi.org/10.1130/G38352.1>.

- Geological Survey of Japan, 1985. Geological Map Hiroshima 1:200,000. Map NI-53-33.
- Glass, B.P., Simonson, B.M., 2013. Distal Impact Ejecta: A Record of Large Impacts in Sedimentary Deposits. Springer-Verlag, Berlin doi:[http://dx.doi.org/10.1007/978-3-540-88262-6\\_716](http://dx.doi.org/10.1007/978-3-540-88262-6_716) p.
- Glasstone, S., Dolan, P.J., 1977. Chapter VII - thermal radiation and its effects, United States Department of Defense and the Energy Research and Development Administration: The Effects of Nuclear Weapons, third ed. 299pp.
- Grima, M., Buttler, M., Hanson, R., Mohameden, A., 2011. Firework displays as sources of particles similar to gunshot residue. *Sci. Justice* 52, 49–57.
- Hermes, R.E., Strickfaden, W.B., 2005. A new look at trinitites. *Nuclear Weapons J.* 2, 2–7.
- Hiroshima Peace Memorial Museum. Virtual Museum, Special Exhibit "It was an atomic bomb. A History of A-bomb Investigations". [http://www.pcf.city.hiroshima.jp/virtual/VirtualMuseum\\_e/exhibit\\_e/exhi\\_fra\\_e.html](http://www.pcf.city.hiroshima.jp/virtual/VirtualMuseum_e/exhibit_e/exhi_fra_e.html).
- Hua, K., Shui, A., Xu, L., Zhao, K., Zhou, Q., Xi, X., 2016. Fabrication and characterization of anorthite-mullite-corundum porous ceramics from construction waste. *Ceram. Int.* 42, 6080–6087.
- Imanaka, T., 2011a. Initial process of atomic bomb cloud formation and radioactivity distribution. In: Aoyama, M., Oochi, Y. (Eds.), Revisit the Hiroshima A-Bomb with a Database: Latest Scientific View on Local Fallout and Black Rain, , pp. 1–14.
- Imanaka, T., 2011b. Radiation survey activities in the early stages after atomic bombing in Hiroshima. In: Aoyama, M., Oochi, Y. (Eds.), Revisit the Hiroshima A-Bomb with a Database: Latest Scientific View on Local Fallout and Black Rain, , pp. 69–81.
- Kerr, G.D., Young, R.W., Cullings, H.M., Christy, R.F., 2005. Bomb parameters. In: Young, R.W., Kerr, G.D. (Eds.), Reassessment of the Atomic Bomb Radiation Dosimetry for Hiroshima and Nagasaki - Dosimetry System 2002, 1, , pp. 2–61.
- Koeberl, C., 2014. The geochemistry and cosmochemistry of impacts, second edition. In: Holland, H.D., Turekian, K.K. (Eds.), Treatise on Geochemistry, vol. 2. Elsevier, Oxford, pp. 73–118 (Planets, Asteroids, Comets and The Solar System).
- Koeberl, C., Hagen, E.H., 1989. Extraterrestrial spherules in glacial sediment from the Transantarctic Mountains, Antarctica: Structure, mineralogy, and chemical composition: undefined. *Geochim. Cosmochim. Acta* 53 (4), 937–944.
- Kyte, F.T., 2002. Iridium concentrations and abundances of meteoric ejects from the Eltanin impact in sediment cores from Polarstern expedition ANT XII/4. *Deep Sea Res.-II* 49, 1049–1061.
- Mao, H., Hillert, M., Selleby, M., Sundman, B., 2006. Thermodynamic assessment of the CaO-Al<sub>2</sub>O<sub>3</sub>-SiO<sub>2</sub> system. *J. Am. Ceram. Soc.* 89, 298–308.
- Marini, F., Raukas, A., 2009. Lechatelierite-bearing microspherules from Semicoke Hill (Kiviõli, Estonia): contribution to the contamination problem of natural microtektites. *Oil Shale* 26 (3), 415–423. doi:<http://dx.doi.org/10.3176/oil.2009.3.06>.
- Mazda Motor Corp, 2005. Report on the Paint Shop Fire at the Ujina No. 1 Plant. Mazda Social and Environmental Report, pp. 9–12.
- Miao, Z., Li, N., Yan, W., 2014. Effect of sintering temperature on the phase composition and microstructure of anorthite-mullite-corundum porous ceramics. *Ceram. Int.* 40, 15795–15799.
- Miller, C.F., 1964. Biological and Radiological Effects of Fallout from Nuclear Explosions. SRI Project No. 111-1536. 82pp. .
- Morgan, L.A., Schulz, K.J., 2012. Physical Volcanology of Volcanogenic Massive Sulfide Deposits in Volcanogenic Massive Sulfide Occurrence Model. U.S. Geological Survey Scientific Investigations Report 2010-5070 -C, Chapter 5. 36pp. .
- Ohtaki, M., 2011. Re-construction of spatial-time distribution of 'black rain' in Hiroshima based on statistical analysis of witness of survivors from atomic bomb. In: Aoyama, M., Oochi, Y. (Eds.), Revisit the Hiroshima A-Bomb with a Database: Latest Scientific View on Local Fallout and Black Rain, , pp. 131–144.
- Pacold, J.L., Lukens, W.W., Booth, C.H., Shuh, D.K., Knight, K.B., Eppich, G.R., Holliday, K. S., 2016. Chemical Speciation of U, Fe, and Pu in Melt Glass From Nuclear Weapons Testing. LLNL-JRNL-681003. 21pp. doi:<http://dx.doi.org/10.1063/1.4948942>.
- Porritt, L.A., Russell, J.K., Quane, S.L., 2012. Pele's tears and spheres: examples from Kilauea Iki. *Earth Planet. Sci. Lett.* 333-334, 171–180. doi:<http://dx.doi.org/10.1016/j.epsl.2012.03.031>.
- Risbud, S.H., Pask, J.A., 1978. Mullite crystallization from SiO<sub>2</sub>-Al<sub>2</sub>O<sub>3</sub> melts. *J. Am. Ceram. Soc.* 61, 63067.
- Sawaki, D., Matsumoto, S., Okubo, T., 2009. Quality of concrete of RC building built at Hiroshima City in early Showa era and its deterioration by atomic bomb. *Cem. Sci. Concr. Technol.* 63, 340–346.
- Stoffler, D., Grieve, R.A.F., 2007. Impactites, chapter 2.11. In: Fettes, D., Desmons, J. (Eds.), Metamorphic Rocks: A Classification and Glossary of Terms, Recommendations of the International Union of Geological Sciences, Cambridge University Press, Cambridge, UK, 82-92, 111-125, and 126-242. .
- Takeoka, H., 2002. Progress in Seto Inland Sea Research. *J. Oceanogr.* 58, 93–107.
- Tamura, N., 2014. XMAS: a versatile tool for analyzing synchrotron X-ray microdiffraction data. In: Ice, G.E., Barabash, R. (Eds.), Strain and Dislocation Gradients from Diffraction. Imperial College Press, London, pp. 125–155.
- Taylor, S., Lever, J.H., Harvey, R.P., 2000. Numbers, types, and composition of an unbiased collection of cosmic spherules. *Meteorit. Planet. Sci.* 35, 651–666.
- U.S. Strategic Bombing Survey, 1946. The Effects of Atomic Bombs on Hiroshima and Nagasaki, Vol. 3. Chairman's Office 46pp.
- Wasson, J.T., 2003. Large aerial bursts: an important class of terrestrial accretionary events. *Astrobiology* 3 (1), 163–179.
- Waters, C.N., Syvitski, J.P.M., Gałuszka, A., Hancock, G.J., Zalasiewicz, J., Cearreta, A., Grinevald, J., Jeandel, C., McNeill, J.R., Summerhayes, C., Barnosky, A., 2015. Can nuclear weapons fallout mark the beginning of the Anthropocene Epoch? *Bull. At. Sci.* 71 (3), 46–57.
- Weisz, D.G., Jacobsen, B., Marks, N.E., Knight, K.B., Isselhardt, B.H., Matzel, J.E., Weber, P.K., Prussin, S.G., Hutcheon, I.D., 2017. Deposition of vaporized species onto glassy fallout from a near-surface nuclear test. *Geochim. Cosmochim. Acta* 201, 410–426.
- Williamson, T.L., Steiner, R.E., Kinman, W.S., Tenner, T.J., Bonamici, C.E., Pollington, A. D., 2016. Determination of Volatility and Element Fractionation in Glassy Fallout Debris by SIMS LA-UR-16-23310. . <http://permalink.lanl.gov/object/tr?what=info:lanl-repo/lareport/LA-UR-16-23310>.
- Witke, J., Weaver, J.C., Bunch, T.E., Kennett, J.P., Kennett, D.J., Moore, A.M., Hillman, G.C., Tankersley, K.B., Goodyear, A.C., Moore, C.R., Daniel, I.R., Ray, J.H., Lopinot, N.H., Ferraro, D., Israde-Alcántara, I., Bischoff, J.L., DeCarli, P.S., Hermes, R.E., Kloosterman, J.B., Revay, Z., Howard, G.A., Kimbel, D.R., Kletetschka, G., Nabelek, L., Lipo, C.P., Sakai, S., West, A., Firestone, R.B., 2013. Evidence for deposition of 10 million tonnes of impact spherules across four continents 12,800 y ago. *Proc. Natl. Acad. Sci. U. S. A.* 110, E2088–E2097.
- Zhang, R., Hayakawa, N., Hosoyamada, T., Sun, Z., 2003. Numerical simulation of the tidal flow around Hiroshima Bay. International Conference on Estuaries and Coasts (November 9-11, 2003, Hangzhou, China), , pp. 358–364.